Journal of Electrical Engineering and Automation (ISSN: 2582-3051)
www.irojournals.com/iroeea/

Frequency and Voltage Stability of Distribution Network using Photovoltaic Stabilization System and Battery Storage System

A. Ebadi Zahedan[1], F. Adabi[2], S. Soleymani[3]

[1,3]Department of Electrical Engineering, Faculty of Mechanics, Electrical and Computer, Science and Research Branch, Islamic Azad University, Tehran, Iran.
[2]Department of Electrical Engineering, Faculty of Engineering, Islamic Azad University, Sanandaj, Iran.

E-mail: [1]alireza.ebadi@srbiau.ac.ir, [2]farid.adabi@iausdj.ac.ir, [3]s.soleymani@srbiau.ac.ir

Abstract

In a power system, various factors such as changes in generator output power due to load changes and different types of short circuits may change the network frequency/voltage as a consequence of changes in network condition. These volatilities in frequency/voltage may cause system frequency/voltage instability. Among different devices used for power system stability, stabilizers are the most important equipment for network stabilization and generator synchronization. In this paper, a photovoltaic system accompanied by battery storage system is used to improve the power system stability following voltage/frequency sudden variations as a result of unpredicted events in the distribution network. To do that, an IEEE 14-bus standard test network is simulated in MATLAB/Simulink, and the performance of the proposed system after different common disturbances is investigated. The results verify the performance of the proposed stabilizer so that it maintains the system stability successfully with zero percent deviation from the original state of the network.

Keywords: Frequency and voltage stability, Synchronous generator, PV system, PI controller, Network synchronization, MPPT (Maximum power point tracking)

1. Introduction

Nowadays, due to technical as well as environmental reasons, photovoltaic (PV) systems are widely used in the distribution networks as Distributed Generation (DG) units. In this paper, a novel scheme that consists of a PV system and suitable battery storage system is

DOI: https://doi.org/10.36548/jeea.2022.4.004
Received: 11.11.2022, received in revised form: 23.11.2022, accepted: 06.12.2022, published: 16.12.2022

used as a network frequency/voltage stabilizer. As a matter of fact, due to economic reasons, power plants operate at their highest capacity and the occurrence of small disturbances or fluctuations can imbalance the total power generation and consumption. On the other hand, because of high inertia of large power plants, their controllers are not well able to return the system to its normal condition by increasing/decreasing the instantaneous production capacity of the system.

The continuation of the power imbalance between system total generation and load may lead to the frequency instability, hence in this paper, the proposed PV and storage system are intended to be sensitized to active power to meet the network power balance constraint and damp the system frequency oscillations. As mentioned, the cause of frequency instability also comes back to the power imbalance between PV production and the grid. After solving the faults and injecting active power into the network, it increases the input power to the generators and Pm>Pe. According to the oscillation equation (equation 1), by integrating both sides of the equation, $\omega>0$, and as a result, the frequency of the network increases. So, the battery receives the extra power from the network and stores it in itself. The reduced voltage is also increasing as a result of active power injection by the proposed system, and as a result, it reaches its initial value. At the moment the fault is resolved, the voltage is still increasing due to the power injection, and at the same moment, the proposed system detects the overvoltage on bus 14 and reduces the voltage value at the same time as the frequency decreases, by reducing the power injection and returns the voltage value to its initial value and makes it stable.

Section 2 presents related works. Section 3 introduces the proposed method. Section 4 presents the simulation results of the scenarios and discusses the comparison of the results in the presence of the proposed system and without the presence of the proposed system. Finally, conclusions are drawn in the last section.

2. Related Works

In normal operation, solar generators do not have an effect on frequency; because they do not have the ability to sense frequency changes. But today, an idea is to make them sensitive to frequency change by measuring the frequency of the network and installing an active power controller on them, thus enabling them to participate in frequency compensation. Due to the high investment cost of PV systems and their use of a free energy source to produce electrical energy, the MPPT system is often used to maximize its financial

return [1]. In [2], CDMPC was used for LFC (Load Frequency Control) of an integrated power system that consists of three areas including a solar power plant, a thermal power plant and a diesel power plant. Since in large-scale power systems, frequency deviations occur due to power fluctuations, in [3] a fast frequency response and damping control of power fluctuations by large-scale solar power plants controlled by STATCOM, known as PV-STATCOM was presented. This technique simultaneously adjusts the frequency and improves the small signal stability of power systems. This controller itself consists of two other controllers: 1) POD (Power Oscillation Damping) controller which is based on reactive power modulation and 2) FFR (Fast Frequency Response) controller which is based on active power modulation. Both of these controllers are used at PV-STATCOM plant level.

In [4] an LFC scheme with sliding mode technique was used in an interconnected multi-zone power system consisting of wind turbines. The LFC is decentralized and designed to ensure the overall stability of the closed loop system. In [5], a controller based on the Super-Twisting algorithm was used for load frequency control of two power systems that are connected nonlinearly and with disturbance. This controller reduces the frequency changes, tie-line error and ACE (Area Control Error) even in case of failure, at a much higher speed than the integral PID controller and brings it to zero. A novel method was used to improve the inertia of the grid using a PV farm with a HESS consisting of a battery and a capacitive supercharger [6]. This method shows the grid dynamics by inverting the inverter voltage angle, and an error-based control was designed to adjust the frequency. For this purpose, PV and HESS were integrated in a common DC connection that was powered by a three-phase VSI (Voltage Source Inverter). A microgrid with a synchronous generator and an energy storage source was also recently being studied. The method of controlling this microgrid is similar to conventional power grids, because by changing the balance of production and consumption, the rotation frequency of the synchronous generator changes and it can be used to control the production of synchronous generators [7, 8].

In article [9], a developed LFC model that supports grid-forming inverters along with the combination of IBG (Inverter-Based Generation) shared with GSS (Grid Support Services) capabilities, was introduced and deals with methods for frequency-load stabilization. Paper [10] dealt with the design of AGC (Automatic Generation Control) of an interconnected thermal power system consisting of three zones, including two thermal generators and a non-linear turbine, by conventional control structures such as PID, PID-N and Fuzzy-PID.

The VSG (Virtual Synchronous Generator) control technique is widely used for the integration of grid-connected renewable energy sources. However, if the VSG is connected to a weak network, it may cause voltage and frequency instability. In research [11], an enhanced control method with inertial damping was presented to increase the frequency stability margin. Today, VI (Virtual Inertial) control is an attractive and effective idea to increase the frequency stability of systems powered by renewable energy. The VI source was created by an inverter-based energy storage system that can correctly imitate the important behaviours of the synchronous generator in terms of inertia and damping characteristics and increase the frequency stability of the entire system. In research [12], the dynamic behaviour of a number of VIs in an interconnected system, in two islanded and grid connected (on-grid) mode has been investigated. The obtained results showed that the instability in the grid-connected mode can be solved by developing multiple VI control.

3. Proposed Work

The oscillation equation of a generator is as follows:

$$2H\frac{d\omega}{dt} = P_m - P_e \tag{1}$$

Where H is inertia constant, ω is generator speed, P_m is input mechanical power to rotate rotor and P_e is generated output electrical power by generator.

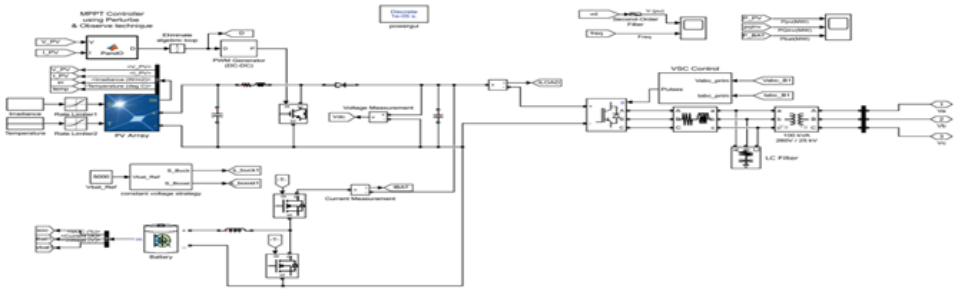

Figure 1. Schematic of the proposed system

According to equation 1, while the input and output power of the generator are equal, $d\omega/dt$ would be zero and the rotor rotates at a constant speed or frequency. As P_e has a direct relation with the current and voltage, changes in the network condition i.e., voltage and current following to a short circuit, results in system frequency oscillation. In the following sections, different parts of under studied system are presented. The schematic of the proposed system is shown in Fig. 1.

3.1 Inverter Control

The interface between the DC link and the AC loads is a three-phase VSI. The high frequency harmonics generated on the side where the load is connected to the VSI can be removed with an LC filter [13]. In a system with PV generation and battery storage system in isolated mode, the inverter must supply the load with the desired voltage range and frequency. The schematic diagram of vector control based on synchronous reference frame is shown in Fig. 2.

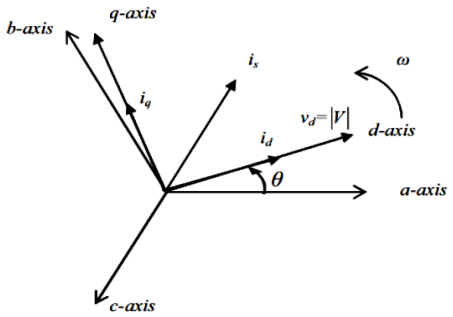

Figure 2. Synchronous reference frame

In this study, ignoring the rotating part of the generator, the frequency and voltage deviations following to a fault is investigated in the synchronous reference frame. In the synchronous reference frame, the system three-phase signals are transformed to DC signals and the systems can be controlled more easily.

The ω is obtained based on the desired frequency of the load voltage and is used to control the system. The load voltage can be written as in equation 2.

$$\begin{bmatrix} v_a \\ v_b \\ v_c \end{bmatrix} = R_f \begin{bmatrix} i_a \\ i_b \\ i_c \end{bmatrix} + L_f \frac{d}{dt} \begin{bmatrix} i_a \\ i_b \\ i_c \end{bmatrix} + \begin{bmatrix} v_{a1} \\ v_{b1} \\ v_{c1} \end{bmatrix} \tag{2}$$

Where L_f and R_f are the inductor and resistor of the LC filter, respectively, v_{a1}, v_{b1} and v_{c1} are the inverter output voltage and i_a, i_b and i_c are the line current.

Using d-q converter, load voltage in the synchronous reference frame would be:

$$v_d = v_{di} - R_f i_d - L_f \frac{di_d}{dt} + \omega L_f i_q \tag{3}$$

$$v_q = v_{qi} - R_f i_q - L_f \frac{di_q}{dt} + \omega L_f i_d \tag{4}$$

Consequently the active and reactive power would be:

$$P = \frac{3}{2}(v_d i_d + v_q i_q) \tag{5}$$

$$Q = \frac{3}{2}(v_d i_q + v_q i_d) \tag{6}$$

If in the synchronous reference frame, v_q and v_d are in the form of $v_q = 0$, $v_d = |V|$ is considered, and equations 5 and 6 are changed to equations 7 and 8.

$$P = \frac{3}{2}(v_d i_d) = \frac{3}{2}|V| i_d \tag{7}$$

$$Q = \frac{3}{2}(v_d i_q) = \frac{3}{2}|V| i_q \tag{8}$$

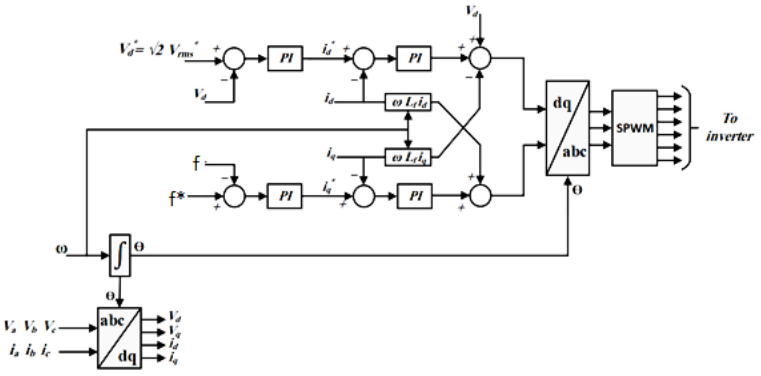

Figure 3. Inverter controlling scheme

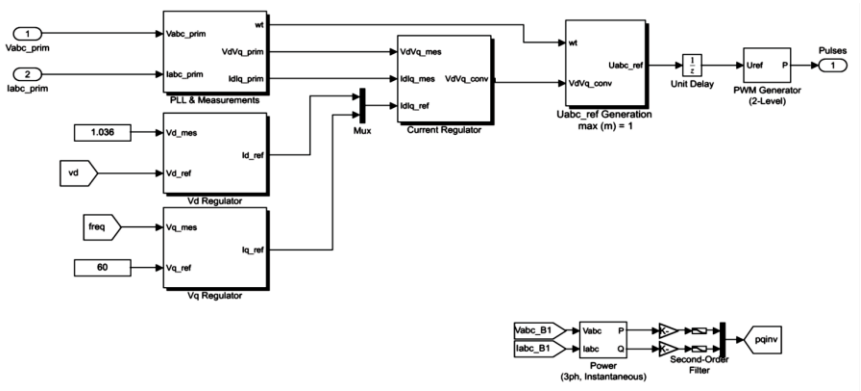

Figure 4. VSC Control scheme

To control the inverter, the reference voltage of axis d, V_d^* is set equal to the desired voltage of the load and the reference axis q as well as the frequency. The inverter controlling diagram is shown in Fig. 3, where there are an external voltage control loop and an internal current control loop. Both controllers are PI type. According to Fig. 4, first, the phase and frequency of the network with PLL is obtained, so that the three-phase signals can be transmitted to the dq0 frame. According to the VSC control block, the output of the voltage

controller is put on the Id_ref axis and the output of the frequency controller on the Iq_ref axis, and with a Multiplexer these two signals are converted into one signal. Then, the reference Idq current is compared with the measured Idq current and added to the measured Vdq signal to obtain the amount of voltage generated by the inverter. After obtaining this voltage, a converter is used to return the signals from qd0 to abc. Now, these three-phase signals are given to a PWM generator to be compared with triangular signals. At any point where the sine values are greater than the value of the triangular signal, the upper switch is turned on and the lower switch is turned off and at any point where the sine values are lower than the value of the triangular signal, the lower switch is turned on and the upper switch is turned off. Thus, the control of the inverter has been completed.

3.2 Photovoltaic System

The structure of photovoltaic systems can be implemented in different ways. In general, these structures are as shown in Fig.5. This structure can be divided into three parts: solar panel, DC-DC converter and MPPT system.

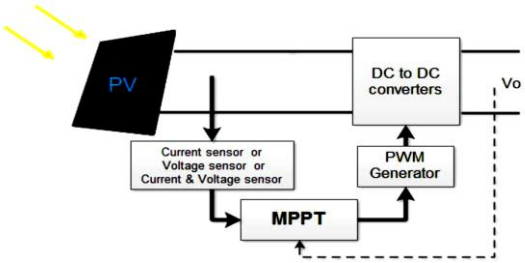

Figure 5. Block diagram of solar power generation system

3.2.1 Solar Panel

The PV system is a nonlinear device that can be considered as a current source as shown in Fig. 6.

$$V_{pv} = \frac{T_{cell}}{q/_{nk}} \times Ln\left(\frac{I_L - I_{pv} + I_s}{I_s}\right) - r_s I_{pv} \tag{9}$$

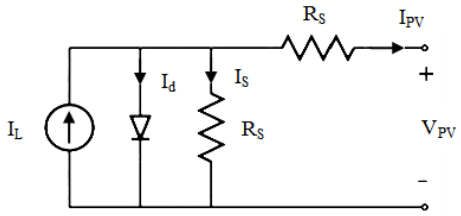

Figure 6. Equivalent circuit of PV cell

The I-V specification of the diode of a single module is defined by:

$$\mathrm{I_d} = \mathrm{I_o}\left[exp\left(\frac{V_d}{V_T}\right) - 1\right] \tag{10}$$

$$V_{pv}^{c} = V_T = \frac{kT}{q} \times nl \times N_{cell} \tag{11}$$

$$I_l = \alpha_1 L \tag{12}$$

For the maximum power point voltage ($\mathrm{V_{mpp}}$), the output power ($\mathrm{P_O}$) relative to the voltage must be derived and set to zero. The voltage obtained from this relation is the maximum power point voltage ($\mathrm{V_{mpp}}$).

$$\frac{\partial P_O}{\partial \mathrm{V_{pv}}} = 0 \rightarrow \mathrm{V_{PVmpp}} = \mathrm{f_1}(L, T_{cell}) \tag{13}$$

Where,

V_{pv}	Solar cell output voltage
$\mathrm{I_d}$	diode current (A)
$\mathrm{V_d}$	diode voltage (V)
Io	saturation diode current (A)
nl	diode ideality factor, a number close to 1.0
I_{pv}	Solar cell output current
T_{cell}	Cell temperature (K)
q	Electron electric charge = 1.6022e-19 C
k	Boltzman constant = 1.3806e-23 J.K-1
n	Dissemination factor
I_{S}	Reverse saturation current
I_{L}	Current depending on the intensity of radiation
r_{s}	Cell series resistance

As a result, the relationship between the point voltage of the maximum output power can be considered as a function of the intensity of L radiation and cell temperature. The operation of PV cells to generate power and inject it into the grid as in Fig. 7, usually takes place in zone 3, which is used to achieve the maximum power produced by the PV cell using MPPT methods.

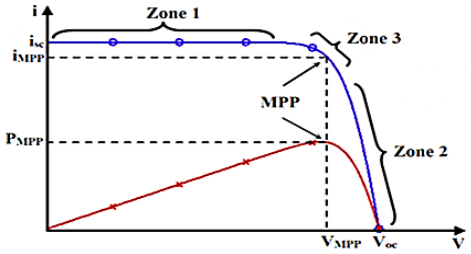

Figure 7. V-I and P-V characteristics of a PV cell (MPPT)

First, a MATLAB function block as in Fig. 8 is used to communicate between the variables defined in the coding section or the MATLAB editor with the variables defined in the Simulink section.

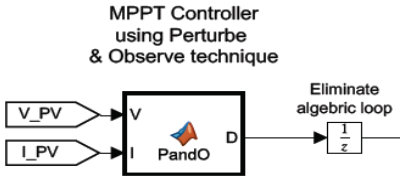

Figure 8. MATLAB function block related to MPPT controller using P & O method

Then, in this block, the duty cycle values, which must be between zero and one, are defined. The minimum and maximum values of duty cycle are equal to 0.001 and 0.999 respectively, and the initial value of duty cycle is equal to 0.45. Some variables are then defined for voltage and power. An initial value (V_{old} and P_{old}) is defined for them and changing these values is not intended. Then, the PV voltage and current values are given to the PV controller block and the power value is calculated according to the equation P=V.I. Then, the two variables dV and dP are defined as voltage changes and power changes respectively, which are shown in equations 14 and 15 and Fig. 9.

$$dV = V - Vold \tag{14}$$

$$dP = P - Pold \tag{15}$$

PV/MPPT Controllerusing Perturbe & Observe technique

```
function D  = PandO(V, I)


Dinit = 0.45;
Dmax = 0.999;
Dmin = 0.001;
deltaD =5e-5;

persistent Vold Pold Dold;

dataType = 'double';

if isempty(Vold)
    Vold=0;
    Pold=0;
    Dold=Dinit;
end
P= V*I;
dV= V - Vold;
dP= P - Pold;
```

Figure 9. Definition **of voltage, power, and duty cycle variable**

Then, a condition with the "if" loop is entered. In this way, if the power changes are zero naturally, as in equation 15, the maximum power has been reached, and this is the best possible state and nothing is done. But if the power and voltage changes are negative, i.e., both are decreasing, the duty cycle must be reduced so that less current goes to the output and as a result, the power decreases. Also, if both changes are positive, still the duty cycle is reduced to reduce the power. If the power changes are positive and the voltage changes are negative, the duty cycle is increased so that, contrary to the previous situation, the current increases and the power increases. In the case where power changes are negative and voltage changes are positive, the same process continues. Complying with all these conditions, a duty cycle is created where the maximum PV power is transferred to the grid.

```
P= V*I;
dV= V - Vold;
dP= P - Pold;

if dP ~= 0
    if dP < 0
        if dV < 0
            D = Dold - deltaD;
        else
            D = Dold + deltaD;
        end
    else
        if dV < 0
            D = Dold + deltaD;
        else
            D = Dold - deltaD;
        end
    end
else D=Dold;
end

if D >= Dmax | D<= Dmin
    D=Dold;
end

Dold=D;
Vold=V;
Pold=P;
```

Figure 10. Conditions related to duty cycle, voltage, and power to find MPP

As shown in Fig. 10, finally, one more condition is added. In this way, if the duty cycle becomes more than the maximum value or less than the minimum value, D is set to the previous value, and then the value of D, V and P are saved for the next loop. As a result, the loop is repeated such that the power is fixed and the maximum power is transferred to the network. So, the switch of the boost converter is set in this way, so that PV gives the maximum power to the grid.

3.2.2 DC to DC Converter

Among different types of DC/DC converters, for photovoltaic system due to the low output voltage boost, voltage converters are typically used. The reason for using the boost converter, in addition to increasing the output voltage of the system, is the variability of the converter input resistance with the duty cycle changes of the applied PWM signal. This feature of the converter gives the ability to change the operating point voltage of the solar cell by changing the operating cycle [14].

3.2.3 Maximum power point tracking method

In this paper, the usual Perturbation and Observation (P&O) method are used to track the maximum power point. The P&O method is the most common algorithm for tracking maximum power due to its simplicity in structure and implementation. In this method, the voltage and current of PV cells are measured and by making a small change in voltage, the received power is compared before and after this change. The direction of this small change in voltage depends on the amount of power measured. If the power measured at the new voltage is higher than the previous state, it will not change to change the voltage, but if the power measured at the new voltage is less than the previous state, it will change to change the voltage.

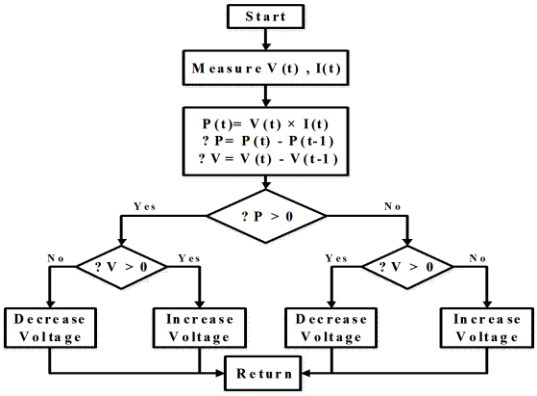

Figure 11. Flowchart of Perturbation and Observation method

For a better understanding, the flowchart of this method is shown in Fig. 11. The P&O method works with a perturbation constant step. The large perturbation step increases the convergence rate but causes swing around the MPP and reduces the efficiency, but the small perturbation step reduces the oscillation around the maximum power point and reduces the convergence rate.

3.3 Battery Storage System

Due to the variability of the produced energy by a PV cell, in some applications, in both grid-connected and off-grid modes, an energy storage element such as a battery is required. Using an energy saver poses challenges in how power is managed between the PV cell, the energy saver, and the consumer. In off-grid applications, due to the fact that the energy from the PV cell is zero during the night and the energy produced during the day is highly variable, according to the radiation conditions and temperature, in order to supply the required energy to the local load continuously, an energy-saving element such as a battery should be used. In such cases, whenever the amount of solar energy exceeds the load

consumption, the excess energy is stored in the battery, and whenever the solar energy is less than the required load, the rest of the energy is supplied by the battery. In some applications to increase system dynamics, in addition to the battery, a super capacitor is used to respond to rapid power changes.

3.4 Control of DC-DC power converter and battery

Energy storage sources such as batteries in isolated microgrids with uncontrolled energy sources are necessary to maintain a balance between production and consumption power. In this article, a lead-acid battery is used for this purpose, which is connected in parallel to a DC link using a DC-DC converter. The main purpose of controlling this converter is to keep the voltage of DC link constant at the reference value, using the internal current control loop with battery charge/discharge. DC-DC dual-feed converter shown in Fig. 12, always operates in continuous conduction mode. The performance of the converter with respect to switches S1 and S2 is in four modes as follows:

- Mode 1 (S2 on): The switch S2 is on, switch S1 is off, and diodes D1 and D2 are in reverse bias, as shown in Fig. 12 (a). In this case, the converter acts as a boost converter and the inductance and current increase.
- Mode 2 (D1 on): Switches S1 and S2 are off and only diode D1 is in direct bias direction (Fig. 12 (b)). In this case, the converter injects battery power into the system.
- Mode 3 (S1 on): In this case, the upper switch S1 is on, the lower switch S2 is off, and the diodes D1 and D2 are in reverse bias, as shown in Fig. 12 (c). In this mode, the converter acts as a tank converter and the power from the system is stored in the battery.
- Mode 4 (D2 on): In this case, switches S1 and S2 are off and only diode D2 is in direct bias (Fig. 12 (d)). In this mode, the energy stored in the inductor in the battery is discharged. In other words, the performance of DC-DC dual-feed converter in the combined system, can be expressed in two ways:

1- Charging mode (Buck): When the DC link voltage value is greater than the DC reference voltage value, the dual-feed converter acts like a buck converter and the battery is charged. In this case, the extra generated power is stored in the battery.

2- Discharge mode (Boost): At low radiation densities, the DC link voltage value is lower than the DC reference voltage value. In this case, the power required by consumers

(network) is more than the output power of the PV system, so the power stored in the battery is transferred to the grid and discharged.

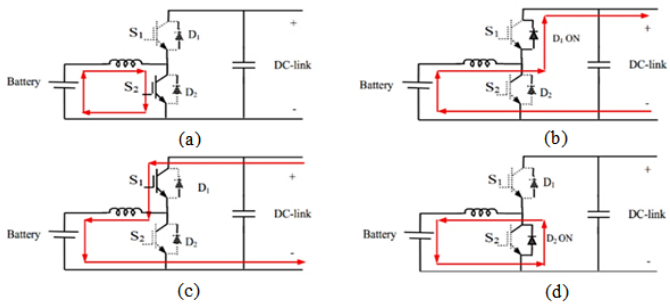

Figure 12. Different modes of operation of DC-DC dual feed converter [13]

Buck-Boost DC-DC dual-feed Converter Control Strategy uses the PI controller for adjusting DC link voltage to the reference value as shown in Fig. 13.

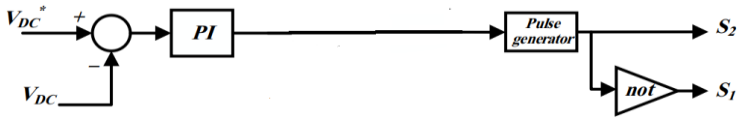

Figure 13. Control of DC-DC dual power converter

In the mentioned control method, DC link voltage is measured and compared with the voltage reference value. Duty cycle of switches S2 and S1 is determined by the output signal for battery charge or discharge modes, and finally the DC link voltage is regulated. In other words, the difference between the DC link voltage and the reference value (battery) is given to the PI controller, and the error is zeroed, and the coefficient ratio is given to it. Next, a PWM block compares the signal given to it (which is a number between zero and one) with a sawtooth or triangle waveform (signal) and compares the constant value that comes out of the PI controller with this sawtooth or triangle signal. Wherever this constant value was greater than the sawtooth or triangular signal, the buck switch (upper switch in Fig. 13) turns on and wherever it was less, using a NOT block, boost switch (lower switch in Fig. 13) turns on. In this way, by this PI controller, the appropriate duty cycle for the switches is produced in such a way that the DC link voltage is always equal to the reference value.

4. Results and Discussion

In this section, three types of errors are considered in three scenarios for the network. The first scenario constitutes a three-phase short circuit fault, the second scenario is a sudden overload in the network and the third scenario is line cutting simultaneously between busses. The fourteenth bus, which has the lowest voltage, has a PV system with a battery that

operates in voltage and frequency control mode and adjusts the voltage and frequency of the fourteenth bus to the reference value. The rated power of PV is considered to be 10MW. Of course, PV needs a DC-DC inverter to be connected to a three-phase network. In this system, the base power is 100MVA, the base voltage is 25kV and the base voltage of the battery is 5kV. Also, the reference frequency is equal to 60Hz and the reference voltage of the fourteenth bus is equal to 1.036p.u. The intensity of sunlight for cells (W/m2) is 1000 and the temperature of cells is 25℃. The results of the simulation for short three-phase connection, overload and line cutting are as follows:

4.1 The 1st Scenario

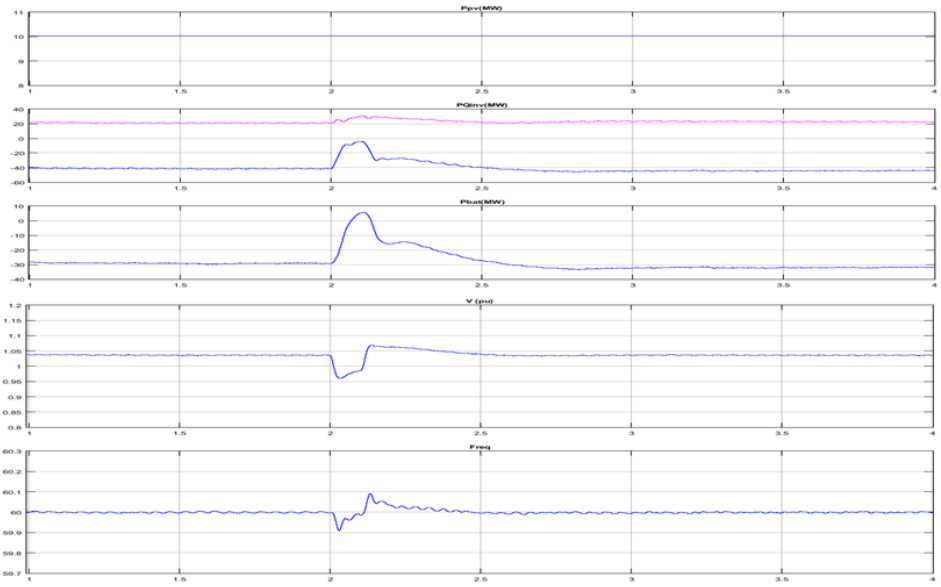

Figure 14. PV output power, active and reactive power of inverter, battery power, 14th bus voltage waveform and frequency waveform in 1st scenario

In this scenario, the short circuit between the three phases occurs at 2.0sec on bus 11 and continues until 2.1sec. The simulation results are as shown in Fig. 14. According to the simulation results in this scenario, before the error occurred, the system is in steady state, the power and frequency are at a constant and initial value, and the battery is charged with a capacity of 30MW due to the lack of network needs. After a short circuit error occurs, due to voltage drop and frequency decrease and according to the relationship $P = V.I\cos\theta$, current and power consumption increase sharply. So the proposed system, by battery, due to the needs of the network, quickly injects all its power into the network and tries to return the voltage to the previous state (1.036p.u.). Until the moment of 2.1sec when the error is fixed and the network suffers from overvoltage and frequency increase, the battery tries to reduce the voltage and frequency to the initial value by storing the extra value. The battery

stores the amount of power that is no longer needed by the grid after fixing the error to prevent overvoltage and increase in frequency, and finally the voltage and frequency after the error are fixed at 1.036p.u. and 60Hz, respectively. Error comparison and zeroing is also done by a simple PI controller.

4.2 The 2nd scenario

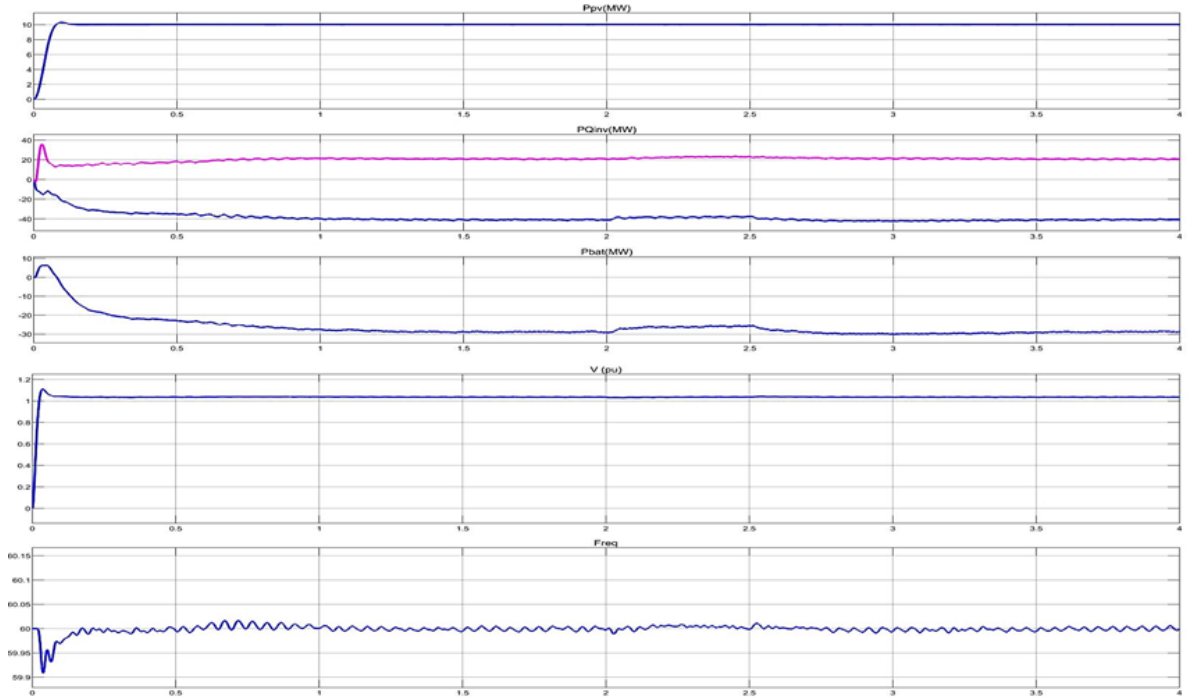

Figure 15. PV output power, active and reactive power of inverter, battery power, 14th bus voltage waveform and frequency waveform in 2nd scenario

In this scenario, a 25MW RLC series is suddenly placed on bus 9 for 2sec by a three-phase breaker and lifted in 2.5sec. The results are shown in Fig. 15. According to the results, it can be seen that the proposed system works properly again and eliminates the excess power generated with proper control, so that the frequency and voltage return to their previous and stable state.

4.3 The 3rd Scenario

In this scenario, the lines between busses 6 and 12 as well as between busses 6 and 13 are cut simultaneously from 2.2sec to 2.6sec for 0.4sec. The results are shown in Fig. 16. According to the results, in all cases, when a short circuit occurs at the same time, the battery quickly supplies the stored energy to the network to compensate for the voltage and frequency drop caused by the short circuit. After fixing the error, the system returns to the previous state.

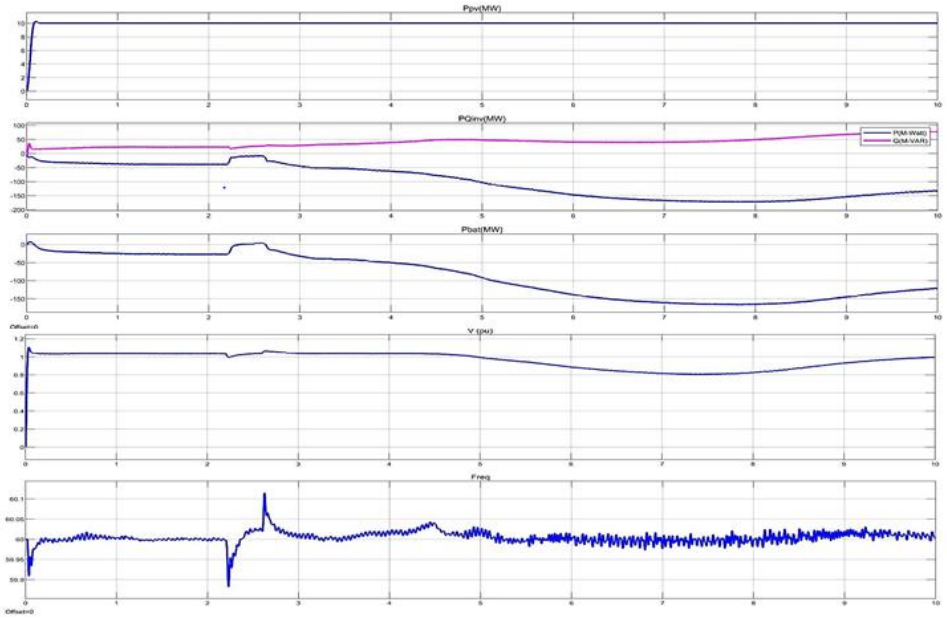

Figure 16. PV output power, active and reactive power of inverter, battery power, 14th bus voltage waveform and frequency waveform in 3rd scenario

4.4 Comparison

The results of scenarios without the proposed system are as follows:

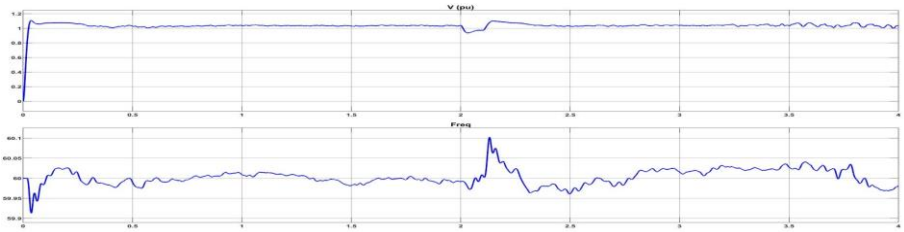

Figure 17. Frequency and 14th bus voltage waveform without proposed system in 1st scenario

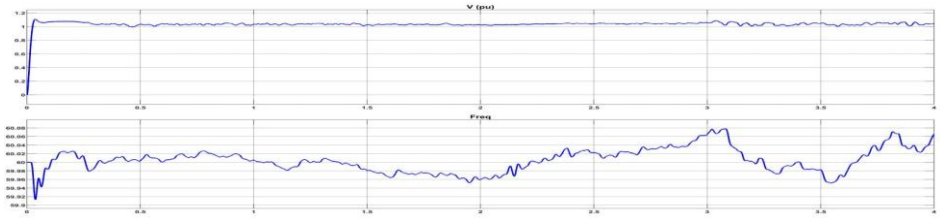

Figure 18. Frequency and 14th bus voltage waveform without proposed system in 2nd scenario

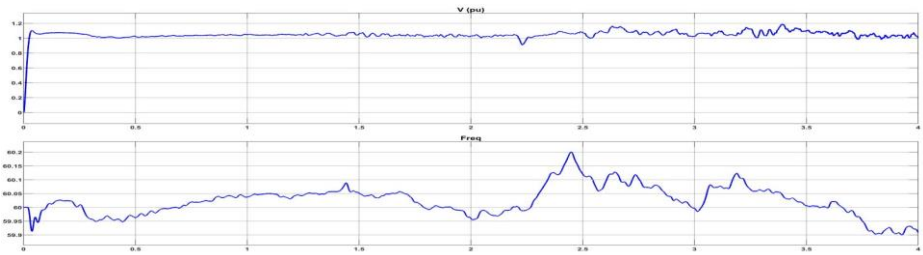

Figure 19. Frequency and 14th bus voltage waveform without proposed system in 3rd scenario

The comparison results of frequency and voltage values are given in Table 1.

Table 1. The comparison results between the proposed system and without the proposed system

Title	First Scenario					
	Before fault		During fault		After fault	
	Freq. (Hz)	Volt. (p.u)	Freq. (Hz)	Volt. (p.u)	Freq. (Hz)	Volt. (p.u)
Values with proposed system	60	1.036	59.90	0.96	60	1.036
Values without proposed system	59.97-60.00	1.036	59.97	0.93	59.96-60.04	1.036
Second Scenario						
Values with proposed system	60	1.036	59.90	1.035	60	1.036
Values without proposed system	59.98	1.036	59.95-60.03	1.036	59.95-60.08	1.00
Third Scenario						
Values with proposed system	60	1.036	59.86	1.00	60	1.036
Values without proposed system	59.95-60.08	1.036	59.96	0.90	59.90-60.20	1.80

4.5 Discussion

Stability of power systems is an important issue that many researchers have researched, tested and proposed various solutions. In this research, special attention has been paid to the issue of frequency and voltage stability and a proposed model including PV system and battery has been presented, which contributes to the frequency stability of the system. The proposed system is implemented on an IEEE 14-bus standard test network, which is shown in Fig. 20 along with various faults.

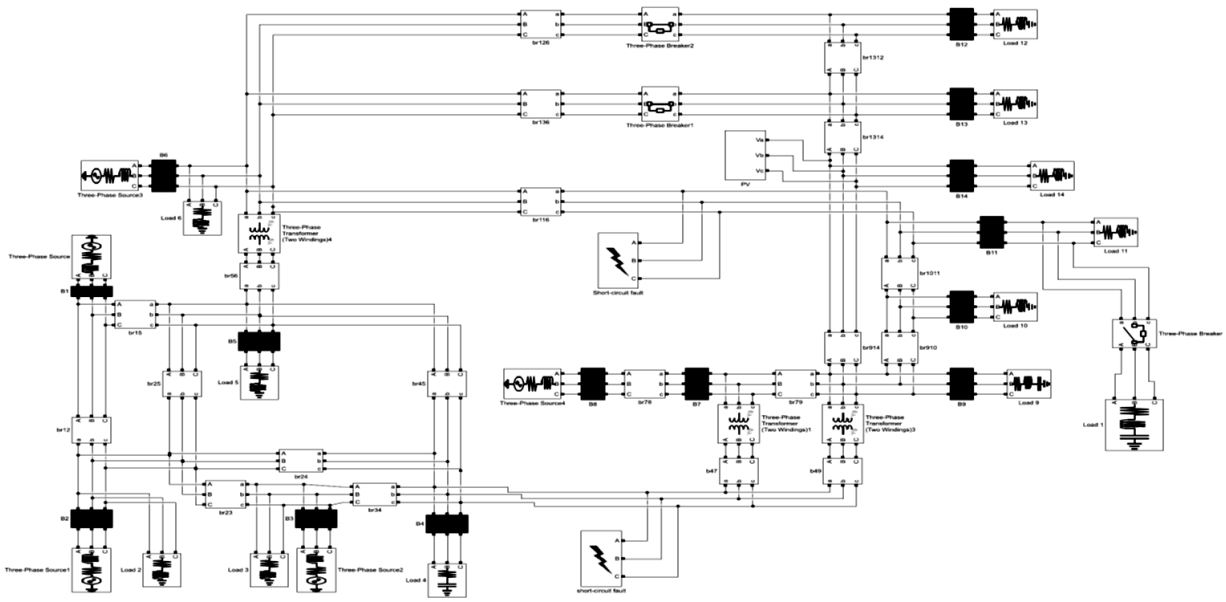

Figure 20. IEEE 14-bus standard test network

5. Conclusion

In this paper, a proposed system based on PV and batteries is presented. First, the generator equations are transmitted to the synchronous reference frame to control the frequency and voltage by voltage and current signals of three-phase DC. The PI controllers then reduce the voltage and frequency error to zero by comparing the reference voltage and frequency value and their value after the faults, and adjust their value to the reference value. The results obtained after the error show that the proposed system performs the task of frequency as well as voltage stability by controlling the active power between the network and PV.

References

[1] Esram, T., Chapman, P., "Comparison of photovoltaic array maximum power point tracking techniques," IEEE Transactions on Energy Conversion, vol. 4, no. 2, p. 413–443, 2117.

[2] X. Liao et al., "Cooperative DMPC-Based Load Frequency Control of AC/DC Interconnected Power System with Solar Thermal Power Plant," 2018 IEEE PES Asia-Pacific Power and Energy Engineering Conference (APPEEC), 2018, pp. 341-346, doi: 10.1109/APPEEC.2018.8566463.

[3] Rajiv K. Varma, M. A. (n.d.). Simultaneous Fast Frequency Control and Power Oscillation Damping by Utilizing PV Solar System as PV-STATCOM. IEEE Transactions on Sustainable Energy .

[4] Yang Mi, Yang Yang, Han Zhang, Aiqing Yu, Limin Wang and Lufei Ren, "Sliding mode based load frequency control for multi-area interconnected power system containing renewable energy," 2014 IEEE Conference and Expo Transportation Electrification Asia-Pacific (ITEC Asia-Pacific), 2014, pp. 1-6, doi: 10.1109/ITEC-AP.2014.6941131.

[5] A. Poulose and R. Kumar P., "Super-Twisting Algorithm based Load Frequency Control of a Two Area Interconnected Power System," 2019 20th International Conference on Intelligent System Application to Power Systems (ISAP), 2019, pp. 1-5.

[6] Joshi, A. Suresh and S. Kamalasadan, "Control and Dispatch of Distributed Energy Resources with Improved Frequency Regulation using Fully Active Hybrid Energy Storage System," 2020 IEEE International Conference on Power Electronics, Smart Grid and Renewable Energy (PESGRE2020), 2020, pp. 1-6.

[7] D. J. Lee and L. Wang, “Small-Signal Stability Analysis of an Autonomous Hybrid Renewable Energy Power Generation/Energy Storage System Part I: Time-Domain Simulations”, IEEE TRANSACTIONS ON ENERGY CONVERSION, VOL. 23, NO. 1, MARCH 2008.

[8] T. Senjyu, T. Nakaji, K. Uezato, and T. Funabashi, “A hybrid power system using alternative energy facilities in isolated island,” IEEE Trans. Energy Convers., vol. 20, no. 2, pp. 406–414, Jun. 2005.

[9] A. Kannan, M. Nuschke and D. Strau-Mincu, "LFC model for frequency stability analysis of prospective power systems with high shares of inverter based generation," 2019 IEEE Milan PowerTech, 2019, pp. 1-6, doi: 10.1109/PTC.2019.8810621.

[10] T. K. Pati, J. R. Nayak, B. K. Sahu and B. Gantayat, "Load frequency control of an interconnected three-area thermal power system using conventional PID & Fuzzy-logic controller," 2015 International Conference on Energy, Power and Environment: Towards Sustainable Growth (ICEPE), 2015, pp. 1-6.

[11] C. Li, Y. Yang, Y. Cao, L. Wang and F. Blaabjerg, "Frequency and Voltage Stability Analysis of Grid-Forming Virtual Synchronous Generator Attached to Weak Grid," in IEEE Journal of Emerging and Selected Topics in Power Electronics, vol. 10, no. 3, pp. 2662-2671, June 2022, doi: 10.1109/JESTPE.2020.3041698.

[12] K. S. Skinder, T. Kerdphol, Y. Mitani and D. Turschner, "Frequency Stability Assessment of Multiple Virtual Synchronous Generators for Interconnected Power System," in IEEE Transactions on Industry Applications, vol. 58, no. 1, pp. 91-101, Jan.-Feb. 2022, doi: 10.1109/TIA.2021.3121219.

[13] M. M. Hussein, T. Senjyu, M. Orabi, M. A. A. Wahab and M. M. Hamada, "Control of a variable speed stand alone wind energy supply system," 2012 IEEE International Conference on Power and Energy (PECon), 2012, pp. 71-76.

[14] Yi-Hua Liu & Jia-Wei Huang ," A fast and low cost analog maximum power point tracking method for low power photovoltaic systems", Solar Energy, Vol. 85,pp. 2771–2780, 13 September 2011.

Author’s biography

Alireza Ebadi Zahedan was born in 1996 in Khalkhal, Ardabil, Iran. He received his Diploma and Pre-university degrees from Ali Ibn Abi Talib high school in Khalkhal in 2014 and 2015, respectively, in mathematics and physics fields with the best ranks. He completed B.Sc. degree in Electrical Engineering with top rank at Urmia University in 2019. He

completed M.Sc. degree in Electrical Engineering Power Systems, at Islamic Azad University, Science and Research Branch, Tehran, Iran in 2022. He is currently working towards a Ph.D. degree in the Department of Electrical Engineering at Urmia University. His fields of interest include Power System Stability, Microgrids, Distributed Networks and Renewable Energies.

Farid Adabi received the B.Sc. degree in electrical engineering from the K. N. Toosi University of Technology, Tehran, Iran, in 2007, the M.Sc. degree in electrical engineering from the Amirkabir University of Technology (Tehran Polytechnic), Tehran, in 2010, and the Ph.D. degree in electrical engineering from the Science and Research Branch of Islamic Azad University, Tehran, in 2016. He is currently an Assistant Professor with Islamic Azad University, Sanandaj Branch, Sanandaj, Iran. His main research interests include smart grid planning and operation, renewable energy systems, electric vehicles as well as electricity market structure and architecture.

Soodabeh Soleymani received the B.Sc. degree in electrical engineering from Sharif University of Technology, Tehran, Iran, in 1999, the M.Sc. degree in electrical engineering from Sharif University of Technology, Tehran, in 2002, and the Ph.D. degree in electrical engineering from Sharif University of Technology in 2009. Currently, she is an Associate Professor in the Department of Power Engineering, Science and Research Branch, Islamic Azad University, Tehran. Her research interests include electrical transients in power systems and power system dynamics.